Highly ordered mesoporous titania with semi crystalline framework templated by large or small nonionic surfactants†

Kevin Zimny,[a] Jaafar Ghanbaja,[b] Cédric Carteret,[c] Marie-José Stébé[a] and Jean-Luc Blin*[a]

Received (in Montpellier, France) 25th June 2010, Accepted 22nd July 2010
DOI: 10.1039/c0nj00488j

A relatively simple and effective route has been developed for the synthesis of mesoporous titania with a high mesopore ordering and thermal stability in short synthetic period (3 days). Mesoporous TiO_2 has been synthesized by a surfactant templating process that combined the evaporation-induced self-assembly method, the liquid crystal templating pathway and basic atmosphere treatment. The developed method can be applied with either large or small surfactants, and in particular with fluorinated ones. The transformation of the amorphous titania walls into nanosized anatase walls occurs without the mesostructure collapse. Moreover, the pore size can be easily tailored by changing the surfactant.

In 1972, Fujishima and Honda discovered the photocatalytic splitting of water on TiO_2 electrodes.[1] This event marked the beginning of a new age in heterogeneous photocatalysis.[2] Since then, photocatalysis using various powdered semiconductors has received much attention for their potential in the utilization of light energy.[2] In particular, research efforts in understanding the fundamental process and in enhancing the photocatalytic efficiency of TiO_2 have come from extensive research due to its low cost, ease of handling and high resistance to photoinduced corrosion.[2–6] Such studies are often related to energy renewal and energy storage, that is to say, that not only has TiO_2 been widely used in the field of photocatalysis, but also has received considerable attention in the applications in electronic, electrochemical systems, including photoelectrochemical solar cells, electrocatalysis, optoelectronic sensor devices and high performance photocatalytic films.[2–6] For the above applications, titania with large surface area and high porosity is favorable.

[a] *Equipe Physico-chimie des Colloïdes, UMR SRSMC No 7565 Université Henri Poincaré-Nancy 1/CNRS, Faculté des Sciences, BP 70239, F-54506 Vandoeuvre-les-Nancy cedex, France. E-mail: Kevin.Zimny@srsmc.uhp-nancy.fr, Marie-Jose.Stebe@srsmc.uhp-nancy.fr, Jean-Luc.Blin@srsmc.uhp-nancy.fr*
[b] *Service commun de microscopie électronique Faculté des Sciences, BP 70239, F-54506 Vandoeuvre-les-Nancy cedex, France. E-mail: Jaafar.Ghanbaja@scmem.uhp-nancy.fr*
[c] *Laboratoire de Chimie Physique et Microbiologie pour l'Environnement UMR7564 Université Nancy 1/CNRS 405, rue de Vandoeuvre, F-54600 Villers-lès-Nancy, France. E-mail: cedric.Carteret@lcpme.cnrs-nancy.fr*

† Electronic supplementary information (ESI) available: Nitrogen adsorption–desorption isotherms and pore size distribution of the recovered titania prepared by using $R^F_8(EO)_9$; P123 and F127 as surfactants (S1). Nitrogen adsorption–desorption isotherms as a function of the calcination temperature (S2). Bright field TEM showing the anatase nanosized crystallite domain after calcination of titania at 350 °C (S3). See DOI: 10.1039/c0nj00488j

TiO_2 can be prepared through different methods,[2] one of them consists in the extension of the surfactant templating process, reported for the preparation of silica mesoporous materials. However, compared to silica materials it is difficult to obtain TiO_2 with stable mesostructure and the main challenge is to preserve the pore ordering upon surfactant removal. Even if most reported studies dealing with ordered mesostructured titania are focused on films,[7–11] some attempts have been made to prepare bulk ordered titania. Ionic surfactants were used initially because their amphiphilic nature provides well-organized micelles around which the titania framework can be assembled by electrostatic interactions.[12,13] However, because of their strong interaction with titania walls, it is very difficult to preserve the structure after the surfactant removal, as the structure generally collapses after the pores are freed from the surfactant by calcination. From this point of view, nonionic surfactants appear as excellent candidates. Indeed due to the weak interactions between the entities, the removal of the surfactant can easily be achieved by solvent extraction, using ethanol for instance.

The other key parameter for the formation of titania with a mesopore ordering concerns the control of the titanium precursor hydrolysis and condensation as well as of the aging process. As a matter of fact precursors such as titanium alkoxides or titanium chloride exhibit a high reactivity towards hydrolysis and condensation. As a consequence, dense TiO_2 with a poor mesopore arrangement is often recovered. To overcome these drawbacks, mixed inorganic precursor[14] or hydrolysis controlling agents, such as actylacetone,[12,15] or hydrogen peroxide,[13] have been used. The self-assembly assisted by block copolymers induced by the controlled evaporation of the solvent (EISA method) also appears to be a promising approach to synthesize mesoporous metal oxides.[16,17] However, in most cases the synthesis of mesoporous titania needs several days (as long as 15 days) and the obtained TiO_2 presents a local organization.

In this paper, we have used a relatively simple and effective route for synthesizing ordered mesoporous titania with a high surface area in a short synthetic period (3 days). Our approach is inspired by the evaporation-induced self-assembly method, which is currently used for the preparation of mesoporous films and the liquid crystal templating pathway that can be employed for the synthesis of silica mesoporous materials.[18,19] This combined method leads to the formation of a hybrid mesophase. A basic treatment under NH_3 atmosphere is required to allow the precipitation of TiO_2. To take benefit of the nonionic surfactant we use liquid crystals of both

polyoxyethylene fluoroalkyl ether and triblock copolymers as mould. To the best of our knowledge this is the first report of a highly ordered titania template by small nonionic surfactants and in particular with fluorinated ones. Moreover, as the method can be applied to different surfactant families, the pore size can be easily tailored.

The used fluorinated surfactant, which was provided by DuPont, has an average chemical structure of $C_8F_{17}C_2H_4$-$(OC_2H_4)_9OH$. It is labeled as $R^F{}_8(EO)_9$. The hydrophilic chain moiety exhibited a Gaussian chain length distribution and the hydrophobic part is composed of a well defined mixture of fluorinated tails. The phase behavior of this surfactant, $R^F{}_8(EO)_9$, was investigated in aqueous solution and subsequently applied to the preparation of mesoporous silicas from both the self-assembly and the liquid crystal pathways.[20,21] Moreover, we have recently shown that liquid crystals of $R^F{}_8(EO)_9$ can be used as a template for the preparation of new TiO_2 films.[10] The films have been self-assembled on a solid substrate by dip-coating using $TiCl_4$ as the titanium source. Their GI-SAXS patterns are characteristic of a 2-D hexagonal structure, in which tubular rods of the fluorinated surfactant are packed hexagonally and aligned parallel to the substrate. Here, to produce bulk ordered TiO_2, we have modified the two synthesis procedures based on the use of $R^F{}_8(EO)_9$ liquid crystals that we have optimized for the preparation of titania films[10] and for the synthesis of silica mesostructures.[21]

Surfactants $R^F{}_8(EO)_9$, P123 and F127 were employed as structure-directing agents, and titanium isopropoxide was used as inorganic precursors. Our approach for the design of highly ordered mesoporous titania is illustrated in Fig. 1 and can be described as follows: the surfactant was first dissolved in a mixture of ethanol and hydrochloric acid (12 N). Then titanium isopropoxide is added before water. The amount of water is fixed in order to keep an acidity of 6 N. Ethanol prevents the formation of a gel and the high concentration of HCl allows the control of the hydrolysis–condensation reactions and avoids the precipitation of a titanium oxide phase. After stirring, in order to form the hexagonal hybrid mesophase, the mixture is placed under vacuum to evaporate the solvent and the propanol produced during the hydrolysis of the titania precursor. The hexagonal symmetry is evidenced by SAXS measurements. For example when P123 is used, lines located at 13.7, 7.8 and 6.6 nm are detected on the pattern (Fig. 2Aa). The relative positions of the Bragg reflections can be attributed to the hexagonal structure. The obtained sample is dried at 40 °C for 12 hours. Afterwards, it is placed in a well-closed glass vessel for 12 hours. The atmosphere of the vessel has been saturated by ammonia vapor. During this step the pH is increased and the condensation reaction occurs. As evidenced

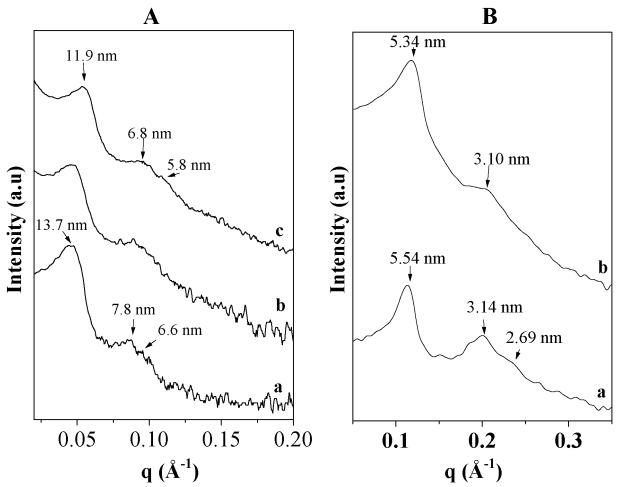

Fig. 2 A: SAXS patterns of TiO_2 prepared with P123; a: after solvent evaporation, b: after treatment with NH_3 and c: after surfactant removal. B: $R^F{}_8(EO)_9$ is used as a surfactant; a: after treatment with NH_3 and b: after surfactant removal.

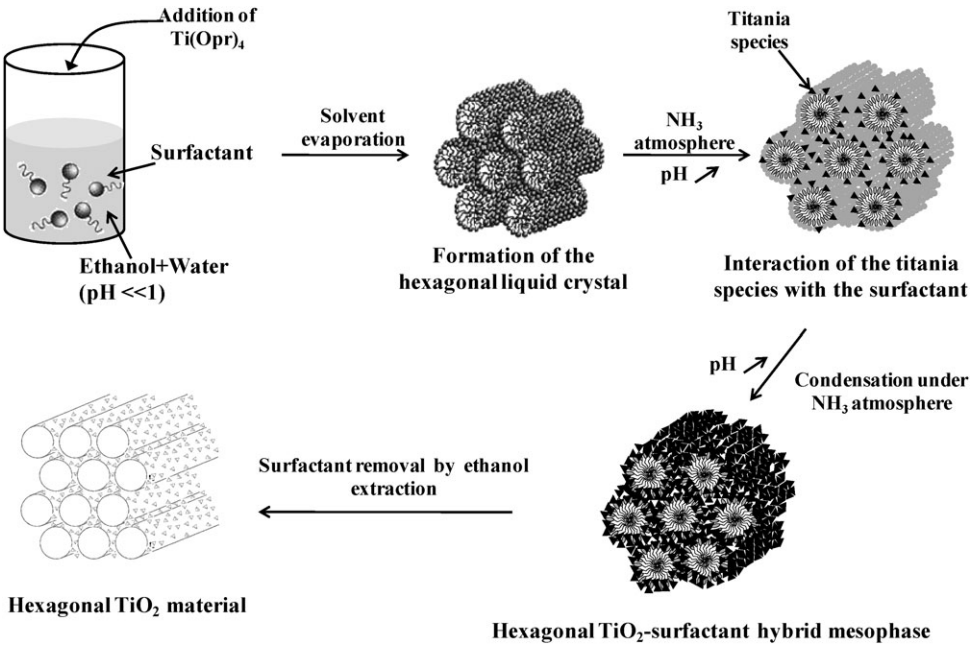

Fig. 1 Different steps of the synthesis of highly ordered mesoporous titania.

in Fig. 2Ab and Ba, the structure is not affected by this treatment.

Finally, almost all of the surfactant species in the product channels are removed by ethanol extraction, which can avoid a possible structural collapse caused during high-temperature calcination to free the pores. As depicted in Fig. 2Ac and Bb, both small [$R^F_8(EO)_9$] and large (P123, F127) surfactants give rise to the preparation of TiO_2 with hexagonal channel array. The mesopore ordering is further confirmed by the transmission electron microscopy (TEM) and the high resolution scanning electron microscopy (SEM) images of different samples (Fig. 3 and 4). Indeed, either the honeycomb like arrangement (Fig. 3a,e and 4a) or the hexagonal stacking (Fig. 3b–d,f and 4b) of the channels is evidenced by the TEM and SEM analysis. The diffraction electron patterns exhibit sixfold symmetry and the measured angles between two bright spots are very close to 60° (Fig. 3a and e, inset). Two light spots (Fig. 3b,c and f, inset) are present, indicative of the parallelism of well oriented channels. The Raman spectra show that the titania frameworks possess amorphous walls. No vibration due to the anatase or rutile is detected. From nitrogen adsorption–desorption measurements (see ESI†, S1), we can observe that whatever the surfactant all the recovered samples exhibit a type IV isotherm, characteristic of mesoporous materials according to the IUPAC classification. By increasing the surfactant size the relative pressure for which capillary condensation takes place is shifted toward higher values. Since the P/P_0 position of the inflection point is related to the pore diameter, it can be inferred that an enlargement of the mean pore diameter occurs when $R^F_8(EO)_9$, P123 and F127 are respectively used, this can be attributed to a larger radius of

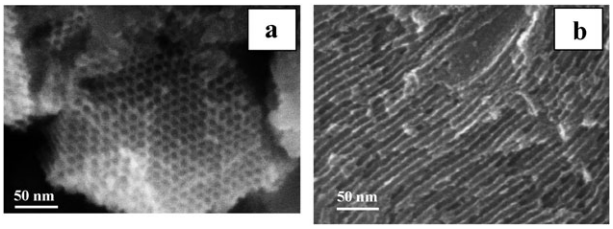

Fig. 4 Representative high resolution scanning electron micrographs of mesoporous TiO_2 showing a high mesopore ordering.

the cylinders composing the liquid crystal phase of the triblock copolymers. This increase in pore diameter is further confirmed by the pore size distribution, whose maximum is shifted from 2.5 [$R^F_8(EO)_9$] to 11.5 nm [F127]. A very high surface area of 370–590 $m^2\ g^{-1}$ can be obtained from this kind of materials' synthesis with different surfactants (Table 1).

Among the common crystalline forms of titania, anatase is generally recognized to be the most active phase. One way to transform the amorphous TiO_2 to anatase consists in calcination. However the main challenge is to preserve the mesostructure upon the calcination process. Indeed, usually the mesostructure of TiO_2 collapses during this treatment. Therefore, we have investigated the thermal stability of the synthesized ordered titania. To perform this study, samples were first heated under nitrogen from 20 °C to the final temperature (ranging from 150 to 550 °C) at a rate of 1 °C min^{-1}. Then, they were kept at this temperature under oxygen for 2 hours. When the calcination temperature reaches 350 °C, both the Raman and the TEM analyses reveal that anatase nanosized crystalline domains are formed in the walls. As a matter of fact the 101, 103, 200, 105,

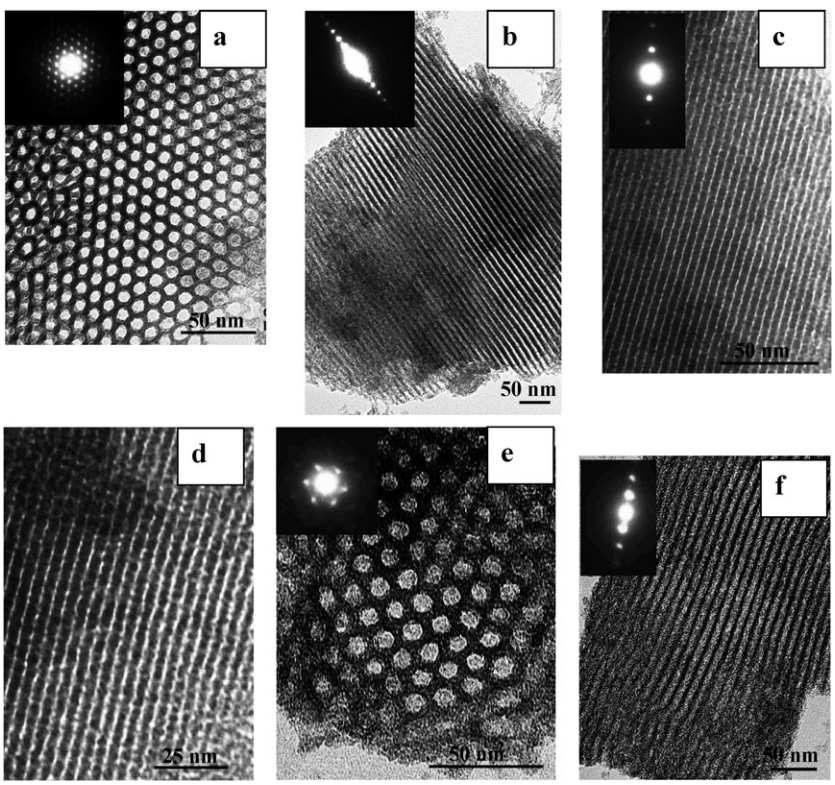

Fig. 3 TEM micrographs of the titania synthesized with P123 (a and b); $R^F_8(EO)_9$ (c and d) and F127 (e and f).

Table 1 Structure, cell parameter (a_0), specific surface area (S_{BET}), pore diameter ($\varnothing$), pore volume (V_p) and wall thickness of the recovered titania

Surfactant	Structure	a_0/nm	S_{BET}/m^2 g^{-1}	$\varnothing$/nm	V_p/cm^3 g^{-1}	Wall thickness/nm
$R^F{}_8(EO)_9$	Hexagonal	6.2	590	2.5	0.30	3.7
P123	Hexagonal	13.7	370	9.8	0.52	3.9
F127	Hexagonal	15.7	457	11.5	0.78	4.2

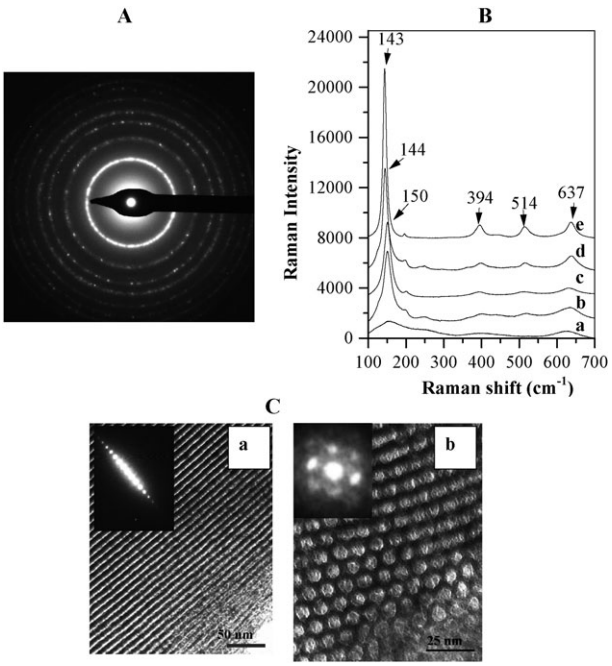

Fig. 5 Characteristics of titania after calcination. A: Electron diffraction pattern showing the formation of the anatase structure. B: Raman spectra of the as-prepared titania (a) and the heat-treated titania at 350 °C (b), 400 °C (c), 450 °C (d). Spectrum of commercial anatase (e) with particle size above 20 nm is given as reference. C: Representative TEM micrographs showing the mesopore ordering after calcination at 400 °C.

213 and 116 reflections of the anatase structure are clearly observed in the electron diffraction pattern (Fig. 5A). In addition in Fig. 5B we show the Raman spectra of TiO_2 mesoporous powders after different heat treatment temperatures. The commercial pure anatase is also shown for comparison. The Raman spectrum of commercial anatase exhibits a very intense band at 143 cm^{-1} (E_g band) and three other bands at 394, 514, and 637 cm^{-1} (B_{1g}, A_{1g} or B_{1g}, and E_g modes, respectively). The Raman spectra of heat-treated mesoporous titania show all the anatase bands. It has been reported that Raman scattering can be used for an estimation of TiO_2 crystallite size, by examining the E_g mode,[22–24] which appears at 143 cm^{-1} in bulk anatase and shifts to higher wavenumbers in nanocrystalline materials. The spectra presented in Fig. 5 show the E_g band at 143 cm^{-1} for the commercial anatase and at 150 cm^{-1} for the material heat-treated at 350 and 400 °C, confirming the presence of nanosized crystallite domain as observed by TEM in dark and bright field (see ESI†, S2). This band shifts to 144 cm^{-1} for the 450 °C thermal-treated TiO_2, as a consequence of the crystallite growth observed during the thermal treatment of the samples. As shown by the TEM micrographs (Fig. 5C) the mesopore ordering is maintained until 450 °C and the complete collapse of the mesostructure appears at 550 °C. Whatever the calcination temperature nitrogen adsorption–desorption isotherms remain type IV (see ESI†, S3). However, the maximum volume of nitrogen adsorbed at relative pressure $p/p_0 = 1$ becomes weaker with the increase of calcination temperature. Its value drops from 370 to 115 cm^3 per g-STP if the calcination temperature is changed from 150 to 550 °C. The specific surface area and the pore diameter also progressively decrease upon calcination. An example of the textural properties variation of a mesoporous TiO_2 with the calcination temperature is reported in Table 2. The sample has been prepared from the P123 surfactant. When the anatase appears the specific surface area still maintains about 80% of its initial value.

In summary mesoporous titania with a high mesopore ordering has been synthesized by a new surfactant templating process that combined both the evaporation-induced self-assembly method and the liquid crystal templating pathway. The developed method can be applied either with large or small surfactants. Moreover, this is the first time that a fluorinated surfactant is used to design mesoporous titania. The obtained mesoporous titania exhibits high thermal stability and the transformation of the amorphous titania walls into nanosized anatase walls occurs at 350 °C without the collapse of the mesostructure. This kind of materials is an excellent candidate for photocatalysis.

Table 2 Cell parameter (a_0), specific surface area (S_{BET}), pore diameter ($\varnothing$), pore volume (V_p) and wall thickness of the titania after calcination

Temperature/°C	TiO_2 structure	a_0/nm	S_{BET}/m^2 g^{-1}	$\varnothing$/nm	V_p/cm^3 g^{-1}	Wall thickness/nm
No calcination	Amorphous	14.1	307	8.8	0.52	5.3
150	Amorphous	14.1	265	7.9	0.44	5.8
250	Amorphous	11.7	272	7.7	0.45	4.0
350	Anatase	11.1	250	7.5	0.40	3.6
400	Anatase	11.1				
450	Anatase	11.1	180	6.4	0.30	4.7
550	Anatase		92	6.4	0.17	—

—, no mesopore ordering.

Experimental section

The fluorinated surfactant was provided by DuPont. The triblock copolymers P123 $(EO)_{20}(PO)_{70}(EO)_{20}$ and F127 $(EO)_{100}(PO)_{70}(EO)_{100}$ were purchased from Aldrich.

Mesoporous titania preparation

In a typical synthesis: 1 g of surfactant is dissolved in 20 g of ethanol under stirring at room temperature. Then 2 g of a hydrochloric acid solution, 3 g of titanium isopropoxide (TiOpr) and 2 g of water are added. The mixture is directly evaporated under vacuum to remove ethanol and isopropanol released by hydrolysis of TiOpr. Samples are dried in an oven at 40 °C for 12 h. Then they are placed under an atmosphere of NH_3 for 12 h to allow the precipitation of TiO_2.

Characterization

SAXS measurements were carried out using a home-built apparatus, equipped with a classical tube (λ = 1.54 Å). The X-ray beam was focused by means of a curved gold/silica mirror on the detector placed at 527 mm from the sample holder. Samples for transmission electron microscopy (TEM) analysis were prepared by crushing some material in ethanol. Afterwards, a drop of this slurry was dispersed on a holey carbon coated copper grid. A Philips CM20 microscope, operated at an accelerating voltage of 200 kV, was used to make the images. N_2 adsorption and desorption isotherms were determined on a Micromeritics TRISTAR 3000 sorptometer at −196 °C. Raman scattering spectra were collected on a Jobin-Yvon T64000 spectrometer equipped with an optical microscope in confocal mode. The excitation beam (514.5 nm) was focused using a long-frontal ×50 objective (numerical aperture 0.5) on an area of about 3 μm^2. The laser power on the sample was approximately 10 mW. The spectral resolution was 3 cm^{-1}, with a wavenumber precision better than 1 cm^{-1}.

Acknowledgements

Authors would like to thank DuPont de Nemours Belgium for providing the fluorinated surfactants. Kevin Zimny thanks the "region Lorraine" for the financial support of his PhD.

References

1 A. Fujishima and K. Honda, *Nature*, 1972, **238**, 37.
2 M. Hoffmann, S. Martin, W. Choi and D. Bahnemann, *Chem. Rev.*, 1995, **95**, 69.
3 M. Fox and M. Dulay, *Chem. Rev.*, 1993, **93**, 341.
4 A. Linsebigler, G. Lu and J. Yates, *Chem. Rev.*, 1995, **95**, 735.
5 T. Thurston and J. Wilcoxon, *J. Phys. Chem. B*, 1999, **103**, 11.
6 X. Chen and S. S. Mao, *Chem. Rev.*, 2007, **37**, 1.
7 D. Grosso, G. J. De A. A. Soller-Illia, F. Babonneau, C. Sanchez, P. A. Albouy, A. Brunet-Bruneeau and A. R. Balkenade, *Adv. Mater.*, 2001, **13**, 1085.
8 J. Yu, J. C. Yu, W. Ho and Z. Jiang, *New J. Chem.*, 2002, **26**, 607.
9 Z. Peng, Z. Shi and M. Liu, *Chem. Commun.*, 2000, 2125.
10 M. J. Henderson, K. Zimny, J. L. Blin, N. Delorme, J. F. Bardeau and A. Gibaud, *Langmuir*, 2010, **26**, 1124.
11 M. J. Henderson, A. Gibaud, J. F. Bardeau and J. W. White, *J. Mater. Chem.*, 2006, **16**, 2478.
12 M. M. Antonelli and J. Y. Ying, *Angew. Chem., Int. Ed. Engl.*, 1995, **34**, 2014.
13 D. T. On, *Langmuir*, 1999, **15**, 8561.
14 B. Tian, H. Yang, X. Liu, S. Xie, C. Yu, J. Fan, B. Tu and D. Zhao, *Chem. Commun.*, 2002, 1824.
15 H. Li, J. L. Shi, J. Liang, X. Li, L. Li and M. Ruan, *Mater. Lett.*, 2008, **62**, 1410.
16 P. Yang, D. Zhao, D. I. Margolese, B. F. Chmelka and G. D. Stucky, *Nature*, 1998, **396**, 152.
17 C. C. Sung, K. Z. Fung, I. M. Hung and M. H. Hon, *Solid State Ionics*, 2008, **179**, 1300.
18 G. S. Attard, J. C. Glyde and C. G. Göltner, *Nature*, 1995, **378**, 366.
19 S. A. El-Safty, Y. Kiyozumi, T. Hanaoka and F. Mizukami, *J. Phys. Chem. C*, 2008, **112**, 5476.
20 J. L. Blin, P. Lesieur and M. J. Stébé, *Langmuir*, 2004, **20**, 491.
21 K. Zimny, J. L. Blin and M. J. Stébé, *J. Phys. Chem. C*, 2009, **113**, 11285.
22 S. Kelly, F. H. Pollak and M. Tomkiewicz, *J. Phys. Chem. B*, 1997, **101**, 2730.
23 W. F. Zhang, Y. L. He, M. S. Zhang, Z. Yin and Q. Chen, *J. Phys. D: Appl. Phys.*, 2000, **33**, 912.
24 A. Pottier, S. Cassaignon, C. Chanéac, F. Villain, E. Tronc and J. P. Jolivet, *J. Mater. Chem.*, 2003, **13**, 877.